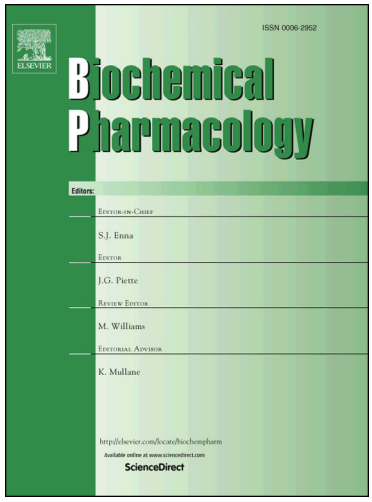

Molecular and functional interaction between GPR18 and cannabinoid CB_2 G-protein-coupled receptors. Relevance in neurodegenerative diseases

Irene Reyes-Resina, Gemma Navarro, David Aguinaga, Enric I. Canela, Clara T. Schoeder, Michal Zaluski, Katarzyna Kiec-Kononowicz, Carlos A. Saura, Christa E. Müller, Rafael Franco

PII: S0006-2952(18)30209-0
DOI: https://doi.org/10.1016/j.bcp.2018.06.001
Reference: BCP 13155

To appear in: *Biochemical Pharmacology*

Received Date: 31 May 2018
Accepted Date: 1 June 2018

Please cite this article as: I. Reyes-Resina, G. Navarro, D. Aguinaga, E.I. Canela, C.T. Schoeder, M. Zaluski, K. Kiec-Kononowicz, C.A. Saura, C.E. Müller, R. Franco, Molecular and functional interaction between GPR18 and cannabinoid CB_2 G-protein-coupled receptors. Relevance in neurodegenerative diseases, *Biochemical Pharmacology* (2018), doi: https://doi.org/10.1016/j.bcp.2018.06.001

Molecular and functional interaction between GPR18 and cannabinoid CB_2 G-protein-coupled receptors. Relevance in neurodegenerative diseases

Running title

Signaling via GPR18 and CB_2 receptors in microglia

Irene Reyes-Resina[a,b], Gemma Navarro[b,c], David Aguinaga[a,b], Enric I. Canela[a,b], Clara T. Schoeder[d], Michal Zaluski[e], Katarzyna Kiec-Kononowicz[e], Carlos A. Saura[b,f], Christa E. Müller[d], Rafael Franco[a,b]

[a]Molecular Neurobiology laboratory, Department of Biochemistry and Molecular Biomedicine, University of Barcelona, Diagonal 643, 08028 Barcelona, Spain

[b]Centro de Investigación en Red, Enfermedades Neurodegenerativas (CIBERNED), Instituto de Salud Carlos III, C/ Sinesio Delgado, 4, 28029 Madrid, Spain

[c]Department of Biochemistry and Physiology. School of Pharmacy. University of Barcelona, Barcelona. Spain.

[d]PharmaCenter Bonn, University of Bonn, An der Immenburg 4, D-53121 Bonn, Germany

[e]Dept. Technology & Biotechnol. of Drugs, Jagiellonian University Medical College, PL 30-688 Kraków, Poland

[f]Institut de Neurociències, Department de Bioquímica i Biologia Molecular, Universitat Autònoma de Barcelona, Campus Bellaterra. Av. Can Domenech, s/n, 08193 Bellaterra, Spain

Corresponding authors

Rafael Franco
Dept. Biochemistry and Molecular Biomedicine
Fac. of Biology. Universitat de Barcelona. Diagonal 643. 08028 Barcelona. Spain
rfranco@ub.edu rfranco123@gmail.com
+34934021208 mobile: +34610306123

Gemma Navarro
Dept. Biochemistry and Physiology
Fac. of Pharmacy. Universitat de Barcelona. Avda Joan XXIII s/n. 08028 Barcelona. Spain
dimartts@hotmail.com
+34934034500

Summary

GPR18, still considered an orphan receptor, may respond to endocannabinoids, whose canonical receptors are CB_1 and CB_2. GPR18 and CB_2 receptors share a role in peripheral immune response regulation and are co-expressed in microglia, which are immunocompetent cells in the central nervous system (CNS). We aimed at identifying heteroreceptor complexes formed by GPR18 and CB_1R or CB_2R in resting and activated microglia. Receptor-receptor interaction was assessed using energy-transfer approaches, and receptor function by determining cAMP levels and ERK1/2 phosphorylation in heterologous cells and primary cultures of microglia. Heteroreceptor identification in primary cultures of microglia was achieved by *in situ* proximity ligation assays. Energy transfer results showed interaction of GPR18 with CB_2R but not with CB_1R. CB_2-GPR18 heteroreceptor complexes displayed particular functional properties (heteromer prints) often consisting of negative cross-talk (activation of one receptor reduces signaling arising from the partner receptor) and cross-antagonism (the response of one of the receptors is blocked by a selective antagonist of the partner receptor). Activated microglia showed the heteromer print (negative cross-talk and bidirectional cross-antagonism) and increased expression of CB_2R and GPR18. Due to the important role of CB_2R in neuroprotection, we further investigated heteroreceptor occurrence in primary cultures of microglia from transgenic mice overexpressing human $APP_{Sw,Ind}$, an Alzheimer's disease model. Microglial cells from transgenic mice showed the heteromer print and functional interactions that were similar to those found in cells from wild-type animals that were activated by treatment with lipopolysaccharide and interferon-ɤ. Our results show that GPR18 and its heteromers may play important roles in neurodegenerative processes.

Keywords

Alzheimer's model, cannabinoid receptor; GPCR heteromer; neurodegeneration; transgenic mice.

Abbreviations

2-AG: 2- arachidonoylglycerol, Abn-CBD: abnormal cannabidiol, AD: Alzheimer's disease, AEA: anandamide, CB_1R: cannabinoid receptor 1, CB_2R: cannabinoid receptor 2, CNS: central nervous system, ERK1/2: extracellular signal-regulated kinase 1/2, MAPK: mitogen-activated protein kinase; NAGLy: *N*-arachidonoylglycine, PLA: proximity ligation assay, PTX: pertussis toxin, Rluc: renilla luciferase, Δ^9-THC: Δ^9-tetrahydrocannabinol.

1. Introduction

GPR18, a GPCR discovered in 1997 (Gantz et al., 1997), is still an orphan receptor although some agonists have been reported. Abnormal cannabidiol (Abn-CBD) is a nonselective GPR18 agonist (Franklin and Stella, 2003); for this reason GPR18 is also known as Abn-CBD receptor. *N*-arachidonoylglycine (NAGly), which arises from anandamide (AEA; *N*-arachidonoylethanolamine) metabolism (Bradshaw et al., 2009), was suggested by (Kohno et al., 2006) and later by (McHugh et al., 2010; Takenouchi et al., 2012; Console-Bram et al., 2014) as the endogenous ligand. In contrast, some authors describe GPR18 as unresponsive to NAGly (Lu et al., 2013; Rempel et al., 2014; Finlay et al., 2016). The receptor became of interest in the cannabinoid research field because cannabinoids may activate it (Járai et al., 1999). In summary, despite potential activation by endocannabinoids and NAGly, GPCR18 still remains as an orphan receptor (IUPHAR/BPS: www.guidetopharmacology.org).

GPR18 is widely expressed in different tissues and cell types. GPR18 expression was first described in spleen, thymus, bone marrow, leucocytes and macrophages (Gantz et al., 1997; Vassilatis et al., 2003; Kohno et al., 2006; Regard et al., 2008; Takenouchi et al., 2012; Becker et al., 2015). However, receptor is also expressed in the central nervous system (CNS) (Vassilatis et al., 2003; Regard et al., 2008; Penumarti and Abdel-Rahman, 2014), in particular in microglia (Walter et al., 2003), in testis, ovary, lungs, intestine (Gantz et al., 1997; Vassilatis et al., 2003), eye (Caldwell et al., 2013) and cancerous cells (McHugh et al., 2010, 2012; Qin et al., 2011).

In the periphery, regulating the immune system, GPR18 is involved in resolving inflammation (Burstein et al., 2011), regulating macrophage apoptosis (Takenouchi et al., 2012) and controlling the fate of intestine intraepithelial lymphocytes following bone marrow

transplantation (Becker et al., 2015). It is also involved in regulating hemodynamic responses (Parmar and Ho, 2010; Penumarti and Abdel-Rahman, 2014; Al Suleimani and Al Mahruqi, 2017; Matouk et al., 2017), cell migration (Walter et al., 2003; McHugh et al., 2010) and intraocular pressure (Miller et al., 2016). Furthermore, its activation produce analgesia (Jeong et al., 2010).

GPR18 is a $G_{i/o}$ coupled receptor, as pertussis toxin (PTX) is able to block the decrease of intracellular cAMP levels elicited by one of the reported agonists, NAGly (Kohno et al., 2006). Intriguingly, it has been described that NAGly, Δ^9-THC and Abn-CBD may increase intracellular Ca^{2+} levels via GPR18, thus suggesting that the receptor is also able to couple to G_q (Kohno et al., 2006; Bradshaw et al., 2009). In addition, activation of GPR18 by NAGly, Δ^9-THC or Abn-CBD may lead to engagement of the MAP kinase pathway in a PTX-dependent fashion (McHugh et al., 2010; Takenouchi et al., 2012). Only Δ^9-THC has been found to recruit ß-arrestins (Yin et al., 2009; Rempel et al., 2014), thus suggesting that the receptor is prone to a markedly biased agonism depending on the structure of the ligand used in the assays.

Endocannabinoids, and natural and synthetic cannabinoids act via specific CB_1 and CB_2 cannabinoid receptors (Lu and Mackie, 2016). Activation of cannabinoid receptors (CB_1R and CB_2R), which are coupled to G_i proteins, leads to an inhibition of adenylate cyclase and a decrease in the intracellular levels of a second messenger, cAMP. The CB_1R is considered as the most abundant GPCR in the CNS, being present in neurons and in glia (Bilkei-Gorzo, 2012); in the CNS the CB_2R is expressed in neurons in some restricted brain areas (see (Lanciego et al., 2011) and references therein) and in glia, mainly in activated microglia (Cabral and Marciano-Cabral, 2005; Fernández-Ruiz et al., 2007). Cannabinoid receptors may establish direct interactions and this may occur in some neurons of the *globus pallidus* where

the two receptors are co-expressed (Callén et al., 2012; Sierra et al., 2015), and in glial cells (Navarro et al., 2018a).

Some authors have described that CB_2R and GPR18 may work in cooperation to regulate microglial cell migration (Franklin and Stella, 2003; Walter et al., 2003). As demonstrated for an increasing number of GPCRs, CB_1R and CB_2R may establish receptor-receptor interactions leading to CB_1R-CB_2R heteromers displaying particular characteristics and with impact on neural regulation of neurotransmission and neuroinflammation (Callén et al., 2012; Navarro et al., 2018a). The two aims of this investigation were to look for potential interactions of GPR18 with cannabinoid CB_1 and/or CB_2 receptors, with a special focus on the CNS, where all three GPCRs are expressed, and to look for the physiological significance of CB_1R/CB_2R-GPR18 heteromer expression and signaling in activated microglial cells, as microglia are the immune competent cells in the CNS. We identified the occurrence of CB_2R-GPR18 heteroreceptor complexes in a heterologous expression system and in primary cultures of microglia in resting conditions and upon activation with LPS and IFN-γ. Functional assays were performed to detect the heteromer print, which was also identified in primary cultures of microglia from a transgenic mouse model of Alzheimer's disease. Microglial cells from the brain of transgenic mice expressed CB_2R-GPR18 receptor complexes that behaved like those in cells from wild-type animals treated with LPS and IFN-γ. These results highlight the potential of GPR18 and CB_2 receptors in microglia for modulating or regulating neurodegeneration and neuroprotection.

2. MATERIALS AND METHODS

2.1. Expression vectors

cDNAs for the human version of CB_1, CB_2, GPR18 and $GABA_B$ receptors with sequences lacking the stop codon were obtained by PCR and subcloned to Rluc-containing vector (pRluc-N1; PerkinElmer, Wellesley, MA) using sense and antisense primers harboring unique restriction sites for HindIII and BamHI, to generate CB_1R-Rluc, GPR18-Rluc and $GABA_B$-Rluc fusion proteins, or subcloned to enhanced yellow fluorescent protein-containing vector (pEYFP-N1; Clontech, Heidelberg, Germany) using sense and antisense primers harboring unique restriction sites for BamHI and KpnI, to generate CB_1R-YFP and CB_2R-YFP fusion proteins, or using sense and antisense primers harboring unique restriction sites for BamHI and HindIII, to generate GPR18-YFP fusion protein.

2.2. Transgenic mouse model of Alzheimer's disease (AD)

$APP_{Sw,Ind}$ transgenic mice (line J9; C57BL/6 background) expressing human APP695 harboring the familial Alzheimer´s disease-linked Swedish (K670N/M671L) and Indiana (V717F) mutations under the PDGFβ promoter were obtained by crossing heterozygous $APP_{Sw,Ind}$ with wild-type (WT) mice (Mucke et al., 2000). Mice at 2 days of age were genotyped individually by conventional PCR (España et al., 2010; Navarro et al., 2018a). Experimental procedures were conducted according to the Animal and Human Ethical Committee of the Universitat Autònoma de Barcelona (protocol CEEAH 1783, Generalitat Catalunya 6381) following the European Union guidelines. Experiments with primary cultures (see below) were performed blindly, without knowing the genotype, which was disclosed for data analysis.

2.3. Cell culture and transient transfection

HEK-293T cells at passage 8-12 were grown in Dulbecco's modified Eagle's medium (DMEM) (Gibco, Paisley, Scotland, UK) supplemented with 2 mM L-glutamine, 100 U/ml penicillin/streptomycin, MEM Non-Essential Amino Acids Solution (1/100) and 50% (v/v)

heat inactivated Fetal Bovine Serum (FBS) (Invitrogen, Paisley, Scotland, UK). Cells were maintained in a humid atmosphere of 5% CO_2 at 37ºC. Cells were transiently transfected with the PEI (PolyEthylenImine, SigmaAldrich) method as previously described (Navarro et al., 2012). To prepare primary microglial cultures, brain was removed from C57BL/6 or $APP_{Sw,Ind}$ mice of 2 days of age. Microglial cells, with a purity >95% purity (according to Iba-1 immunoreactivity and Hoechst nuclei staining) were isolated as described elsewhere (Navarro et al., 2018a) and grown in DMEM medium supplemented with 2 mM L-glutamine, 100 U/ml penicillin/streptomycin, MEM Non-Essential Amino Acids Solution (1/100) and 5% (v/v) heat inactivated Fetal Bovine Serum (FBS) (Invitrogen, Paisley, Scotland, UK). In brief, samples were dissected, carefully stripped off the meninges and digested with 0.25% trypsin for 30 min at 37ºC. Trypsinization was stopped by adding an equal volume of culture medium (Dulbecco's modified Eagle medium-F-12 nutrient mixture, fetal bovine serum 10%, penicillin 100 U/mL, streptomycin 100 µg/mL and amphotericin B 0.5 µg/ml) containing 160 mg/mL deoxyribonuclease I (all those reagents from Invitrogen). Cells were brought to a homogeneous suspension by repeated pipetting followed by passage through a 100 µm-pore mesh and pelleted (7 min, 200 x g). Glial cells were resuspended in medium and seeded at a density of 3.5×10^5 cell/ml in 6-well plates. Cultures were maintained at 37ºC in humid 5% CO_2 atmosphere and medium was replaced at DIV 2 and once every week. For other assays cells were grown either in 6-well plates at a density of 500,000/well in 2 mL or directly in 96-well plates at a density of 50,000/well; each well having a volume of 0.2 ml. For cAMP assays, cells grown on 6-well plates were scrapped and placed in 384-well plates at a density of 2,500 cells/well. Cell counting was assessed using trypan blue and a Countless II FL automated cell counter (Thermo Fisher Scientific-Life Technologies).

Bioluminescence resonance energy transfer (BRET) assays

HEK-293T cells growing in 6-well plates were transiently cotransfected with a constant amount of cDNA encoding for CB_1-Rluc, GPR18-Rluc or $GABA_B$-Rluc and with increasing amounts of cDNA corresponding to CB_2-YFP, CB_1-YFP or CB_2-YFP and GPR18-YFP, respectively. 48 h post transfection cells were washed twice in quick succession in HBSS (137 mM NaCl; 5 mM KCl; 0.34 mM Na_2HPO4; 0.44 mM KH_2PO_4; 1.26 mM $CaCl_2$; 0.4 mM $MgSO_4$; 0.5 mM $MgCl_2$; and 10 mM HEPES pH 7.4) supplemented with 0.1% glucose (w v-1), detached by gently pipetting and resuspended in the same buffer. To assess the amount of cells per plate, protein concentration was determined using a Bradford assay kit (Bio-Rad, Munich, Germany) using bovine serum albumin dilutions as standards. To quantify YFP-fluorescence expression, cells (20 μg protein) were distributed in 96-well plates (black plates with a transparent bottom; Porvair, Leatherhead, UK) and fluorescence was read using a Mithras LB 940 (Berthold, Bad Wildbad, Germany) equipped with a high-energy xenon flash lamp, using a 10-nm bandwidth excitation and emission filters at 485 and 530 nm, respectively. YFP-fluorescence expression was determined as fluorescence of the sample minus the fluorescence of cells expressing protein-Rluc alone. For BRET measurements, the equivalent of 20 μg of cell suspension was distributed in 96-well plates (white plates; Porvair) and 5 μM coelenterazine H (PJK GMBH, Kleinblittersdorf, Germany) was added. 1 min after coelenterazine H addition, readings were collected using a Mithras LB 940 (Berthold, Bad Wildbad, Germany), which allows the integration of the signals detected in the short-wavelength filter at 485 nm (440–500 nm) and the long-wavelength filter at 530 nm (510–590 nm). To quantify receptor-Rluc expression, luminescence readings were performed 10 min after 5 μM coelenterazine H addition. The net BRET is defined as [(long-wavelength emission)/(short-wavelength emission)]-Cf where Cf corresponds to [(long-wavelength emission)/(short-wavelength emission)] for the Rluc construct expressed alone in the same experiment. BRET curves were fitted assuming a single phase by non-linear regression

equation using the GraphPad Prism software (San Diego, CA, USA). BRET values are given as milli BRET units (mBU: 1,000 x net BRET).

2.4. Immunostaining procedures

Cells were fixed in 4% paraformaldehyde for 15 min and washed twice with PBS containing 20 mM glycine before permeabilization with PBS-glycine containing 0.2% Triton X-100 (5 min incubation). HEK-293T cells were treated for 1 h with PBS containing 1% bovine serum albumin and labelled with a mouse anti-Rluc (1/100; MAB4400, Millipore) antibody, and subsequently treated with Cy3-conjugated anti-mouse (1/200; 715-166-150; Jackson ImmunoResearch (red)) IgG secondary antibody (1 h each). Specificity of antibodies was tested in untransfected HEK-293T cells (data not shown). Samples were washed several times and mounted with 30% Mowiol (Calbiochem). Samples were observed in a Leica SP2 confocal microscope (Leica Microsystems).

2.5. cAMP determination

Two hours before adding reagents, HEK-293T cells or microglial primary cultures were placed in serum-free medium. Then, cells were detached and suspended in medium containing 50 µM zardaverine. Cells were placed in 384-well plates (2,500 cells/well), pretreated (15 min) with the corresponding antagonists -or vehicle- and stimulated with agonists (15 min) before adding 0.5 µM forskolin or vehicle (15 min). Readings were performed after 1 h of incubation at 25ºC. Homogeneous time-resolved fluorescence energy transfer (HTRF) measures were performed using the Lance Ultra cAMP kit (PerkinElmer, Waltham, MA, USA). Fluorescence at 665 nm was analyzed on a PHERAstar Flagship plate reader equipped with an HTRF optical module (BMG Lab technologies, Offenburg, Germany). The value of reference (100%) was that achieved by 0.5 µM forskolin treatment. The effect of ligands was given in percentage respect to the reference value.

2.6. ERK phosphorylation assays

To determine ERK1/2 phosphorylation, 40,000 cells/well were plated in transparent Deltalab 96-well plates and kept at the incubator for 48 h. 2 to 4 h before the experiment, the medium was replaced by serum-free medium. Then, cells were pre-treated at 25°C for 10 min with vehicle or antagonists in serum-free DMEM medium and stimulated for an additional 7 min with agonists. Cells were then washed twice with cold PBS before addition of lysis buffer (20 min treatment). 10 µL of each supernatant were placed in white ProxiPlate 384-well plates and ERK 1/2 phosphorylation was determined using AlphaScreen®SureFire® kit (Perkin Elmer) following the instructions of the supplier and using an EnSpire® Multimode Plate Reader (PerkinElmer, Waltham, MA, USA). The value of reference (100%) was that achieved in the absence of any treatment (basal). The effect of ligands was given in percentage respect to the basal value.

2.7. Dynamic mass redistribution (DMR) assays

Cell mass redistribution induced upon receptor activation was detected by illuminating with polychromatic light the underside of a biosensor and measuring the changes in the wavelength of the reflected monochromatic light that is a sensitive function of the index of refraction. The magnitude of the wavelength shift (in picometers) is directly proportional to the amount of mass redistribution. HEK-293T cells were seeded in 384-well sensor microplates to obtain 70-80% confluent monolayers constituted by approximately 10,000 cells per well. Previous to the assay, cells were washed twice with assay buffer (HBSS with 20 mM HEPES, pH 7.15) and incubated 2 h with assay-buffer containing 0.1% DMSO (24°C, 30 µL/well). Hereafter, the sensor plate was scanned and a baseline optical signature was recorded for 10 min before adding 10 µL of the selective antagonists for 30 min followed by the addition of 10 µL of the selective agonists; all test compounds were dissolved in assay buffer. Then, DMR responses

were monitored for at least 5,000 s in an EnSpire® Multimode Plate Reader (PerkinElmer, Waltham, MA, USA). Results were analyzed using EnSpire Workstation Software v 4.10.

2.8. *In situ* proximity ligation assays (PLA)

Microglial primary cultures grown on glass coverslips were fixed in 4% paraformaldehyde for 15 min, washed with PBS containing 20 mM glycine to quench the aldehyde groups and permeabilized with the same buffer containing 0.05% Triton X-100 (5 min treatment). Fixed cells were incubated for 1 h at 37º with blocking solution (from PLA kit, see below) and subsequently treated with specific antibodies against CB_2 (SC-25494 raised in rabbit; 1/100) and GPR18 (SC-79501, raised in goat; 1/100) receptors and processed using the PLA probes detecting rabbit and goat antibodies (Duolink II PLA probe anti-Rabbit plus and Duolink II PLA probe anti-Goat minus). Specificity of antibodies was tested in untransfected HEK-293T cells (data not shown). Duolink II in situ PLA detection kit (Duolink® In Situ Detection Reagents Red, DUO92008, developed by Olink Bioscience, Uppsala, Sweden; and now distributed by SigmaAldrich as Duolink® using PLA® Technology) was used to detect the presence/absence of receptor clusters in the samples, which were incubated with the ligation solution for 1 hour, washed and subsequently incubated with the amplification solution for 100 min (both steps at 37°C in a humid chamber). Nuclei were stained with Hoechst (1/100; SigmaAldrich). Mounting was performed using 30% Mowiol (Calbiochem). Negative controls were performed by omitting the primary anti-GPR18 antibody. Samples were observed in a Leica SP2 confocal microscope (Leica Microsystems, Mannheim, Germany) equipped with an apochromatic 63X oil-immersion objective (N.A. 1.4), and 405 nm and 561 nm laser lines. For each field of view a stack of two channels (one per staining) and 5 Z stacks with a step size of 1 µm were acquired. The number of cells containing one or more red spots versus total cells (blue nucleus) and, in cells containing spots, the ratio r (number of red spots/cell), were determined by means of the Duolink Image tool software.

2.9.Real time (RT)-PCR assay

Total RNA was extracted from primary cultures of microglial cells treated for 48 h with vehicle (cell culture medium) or LPS plus IFN-γ (in medium). Pelleted microglial cells were treated with 1.5 mL of TRIzol Reagent (Thermo Fisher) and 300 µl of chloroform (SigmaAldrich). The aqueous phase containing total RNA was recovered after centrifugation for 15 min at 12,000 x g at 4ºC, mixed with 750 µl of isopropanol (Panreac) and left overnight at -80ºC. Total RNA was then purified by centrifugation at 12,000 x g at 4ºC (15 min), washing the pellet with 70 % ethanol (Panreac) and suspending the final pellet in Milli-Q water. Total RNA was quantified spectrophotometrically using a Nano Drop ND-1000 (Thermo Scientific). Total RNA (1 µg) was reversely transcribed by random priming using the High Capacity cDNA Reverse Transcription Kit from Applied Biosystems (Foster City, CA, USA). The resulting single stranded cDNA was used to perform PCR amplification for CB_2R, and for GAPDH as an internal control using Power SYBR Green PCR Master Mix from Promega (Madison, WI, USA). Fluorescence readouts were collected using a 7500 Fast Dx Real-Time PCR Instrument from Applied Biosystems (Foster City, CA, USA). CB_2R forward primer was: 5'-CATCACTGCCTGGCTCACT-3' and reverse primer was: 5'- AGCATAGTCCTCGGTCCTCA-3'. In the case of GPR18, the forward primer was: 5'-TGAAGCCCAAGGTCAAGGAGAAGT-3' and the reverse primer was: 5'-TTCATGAGGAAGGTGGTGAAGGCT-3'. In the case of GAPDH the forward/reverse primers were, respectively, 5'-CATCCTGCACCACCAACTGCTTAG-3' and 5'-GCCTGCTTCACCACCTTCTTGATG-3'. In the absence of reverse transcription, no fluorescence was detected, thus indicating that there was no genomic DNA contamination. MIQUE guidelines were followed.

2.10. Data analysis

The data in graphs are the mean ± S.D. GraphPad Prism software version 5 (San Diego, CA, USA) was used for data fitting and statistical analysis. One- or two-way ANOVA followed by *post-hoc* Bonferroni test were used depending of the number of factors. Two factors were considered in the case of ligand treatments (8 levels) in resting or activated cells (two levels) or in the case of ligand treatments in microglia from control or transgenic mice (two levels). PLA data in Fig. 5 were analyzed using two-way ANOVA with two levels for each factor (negative/positive and control/transgenic). When pair of values were compared, the Student's t test was used. Significant differences were considered when $p < 0.05$.

2.11. Reagents

LPS and interferon-γ (IFN-γ) were purchased from SigmaAldrich (St Louis, MO, USA) and ACEA, JWH133 and AM630 from Tocris Bioscience (Bristol, UK). PSBKK1415 and PSBCB5 were synthesized in the Department of Technology and Biotechnology of Drugs, Jagiellonian University Cracow, Poland, and provided by Prof. Christa Müller, PharmaCenter Bonn, Bonn (Rempel et al., 2014; Schoeder, 2017).

3. RESULTS

3.1. GPR18 interacts with cannabinoid CB_2 but not with CB_1 receptors

To determine whether GPR18, which belongs to the superfamily of G-protein-coupled receptors, could form heteromeric complexes with cannabinoid CB_1 or CB_2 receptors, an immunocytochemistry assay was first developed to assess the potential colocalization of GPR18 and cannabinoid receptors in cotransfected cells. To do so, the heterologous HEK-293T cell-expression system was used. Cells were transfected with cDNAs for CB_1R-YFP (green, top left panel in Fig. 1A), CB_2R-YFP (green, top center panel in Fig. 1A) or GPR18-

Rluc (red, top right panel in Fig. 1A). Receptor expression was detected by YFP's own fluorescence for CB_1R and CB_2R, or using an anti-Rluc antibody and a secondary Cy3-conjugated antibody for GPR18. As observed in Figure 1A, all three receptors were found in different cell locations including the plasma membrane. Moreover, when HEK-293T cells were transfected with cDNAs for GPR18-Rluc and either CB_1R-YFP or CB_2R-YFP, both GPR18/CB_1R and GPR18/CB_2R showed a significant degree of co-localization (Fig. 1A). Indeed, co-localization does not prove a direct interaction; hence, to demonstrate physical interactions between receptor pairs, a bioluminescence resonance energy transfer (BRET) approach was used. We checked that all cannabinoid and GPR18 receptor-fusion proteins properly trafficked to the cell membrane, as shown by confocal microscopy, and were functional, as shown by similar ability to decrease forskolin-induced cAMP levels as that of native proteins (Fig. 1B). BRET was undertaken in HEK-293T cells expressing a constant amount of cDNA for GPR18-Rluc and increasing amounts of cDNA for CB_1R-YFP. An unspecific linear signal was obtained, indicating the lack of interaction between CB_1 and GPR18 receptors (Fig. 1C). A similar linear relationship was obtained for the negative control consisting of HEK-293T cells expressing a constant amount of $GABA_BR$-Rluc and increasing amounts of GPR18-YFP (Fig. 1E). However, when a similar experiment was developed transfecting HEK-293T cells with a constant amount of cDNA for GPR18-Rluc and increasing amounts of cDNA for CB_2R-YFP, a saturation BRET curve ($BRET_{max}$ 227 mBU, $BRET_{50}$ 47.5) was obtained, thus indicating a specific interaction between GPR18 and CB_2 receptors (Fig. 1D). As positive control, a saturation BRET curve ($BRET_{max}$ 57.9 mBU, $BRET_{50}$ 4.28) was obtained in HEK-293T cells expressing CB_1R-Rluc and increasing amounts of CB_2R-YFP (Fig. 1E). These results indicate that GPR18 may form heteroreceptor complexes with CB_2 but not with CB_1 receptors.

3.2. Functional characterization of CB_2-GPR18 heteroreceptor complexes in HEK-293T cells

It is well established that CB_2R couples to heterotrimeric G_i proteins and its activation inhibits adenylate cyclase thus decreasing intracellular cAMP levels (Lu and Mackie, 2016). Some authors have reported that GPR18 may also couple to G_i (Kohno et al., 2006). Accordingly, we first determined cAMP levels in forskolin-treated HEK-293T cells expressing CB_2R, GPR18 or both. Agonist concentrations were selected from preliminary dose-response experiments in which the ability of JWH133 or PSBKK1415 to decrease forskolin-induced cAMP levels was assayed using HEK-293T cells expressing, respectively, CB_2R or GPR18 (Fig. 2A-B). On the one hand, the selective CB_2R agonist, JWH133 (100 nM), decreased forskolin-induced cAMP levels in HEK-293T cells expressing the receptor, and induced a small non-statistically significant effect in cells expressing GPR18 (Fig. 3A-B). On the other hand, PSBKK1415 (30 nM), a selective GPR18 agonist, induced a significant decrease in cAMP levels in forskolin-treated HEK-293T cells expressing the receptor, while having no effect in CB_2R-expressing cells (Fig. 3A-B). Moreover, the CB_2R selective antagonist, SR144528 (1 μM) inhibited the JWH133 induced effect in CB_2R-expressing cells (Fig. 3A), while PSBCB5 (1 μM), a selective GPR18 receptor antagonist, counteracted the PSBKK1415-induced effect in GPR18-expressing cells (Fig. 3B). In HEK-293T cells expressing both CB_2 and GPR18 receptors, JWH133 decreased cAMP levels in a similar manner to that observed in cells only expressing CB_2R. In contrast, the treatment with PSBKK1415 was ineffective, thus suggesting that the simple expression of CB_2R blocks the PSBKK1415-induced GPR18 activation and signaling. Finally, when cotransfected cells were simultaneously treated with the two agonists, no effect was observed (Fig. 3C). A negative cross-talk may be used as a print to detect the GPR18-CB_2 heteroreceptor complexes in natural sources. Although the pretreatment with GPR18 receptor antagonist PSBCB5 (1 μM)

slightly decreased the JWH133 induced effect in cotransfected cells, no significant differences were found compared to the single treatment with JWH133 (Fig. 3C).

MAPK engagement, which may be mediated by G-protein-independent mechanisms, was also analyzed. Agonist concentrations were selected from dose-response experiments of JWH133 or PSBKK1415 treatments in which ERK1/2 phosphorylation in HEK-293T cells expressing CB_2R or GPR18, respectively, was tested (Fig. 2C-D). In CB_2R-expressing HEK-293T cells it JWH133 specifically increased ERK1/2 phosphorylation, while PSBKK1415 induced no effect (Fig. 3D). In GPR18-expressing cells, PSBKK1415 (30 nM) induced a significant effect while the CB_2R selective agonist had no effect (Fig. 3E). In HEK-293T cells expressing the two receptors both JWH133 and PSBKK1415 induced a small effect when used individually that was reduced when used in combination (Fig. 3F). Accordingly, a negative cross-talk was also observed in MAPK signaling. Interestingly, in cotransfected cells pretreated with the selective CB_2R antagonist SR144528 (1 µM) or with the selective GPR18 receptor antagonist PSBCB5 (1 µM), the effect of both JWH133 and PSBKK1415 on ERK1/2 phosphorylation was counteracted, thus a cross-antagonism effect was detected on both directions (Fig. 3F). Uni- or bi-directional cross-antagonism constitute reliable heteromer prints. DMR, which is a label-free method to measure cellular mass movements induced upon receptor activation, was determined in cells expressing either receptor. JWH133 or PSBKK1415 provided significant real-time DMR recordings by, respectively, activating CB_2R or GPR18 receptors (Fig. 3G-H). Interestingly, the cross-talk and cross-antagonism detected in cAMP determination and MAPK signaling assays were also observed in cells expressing both receptors (Fig. 3I).

These results show receptor heteromerization and a functional cross-talk that is due to the molecular interaction and that is disclosed by negative cross-talk and/or cross-antagonism

3.3. Functional characterization of CB_2-GPR18 heteroreceptor complexes in primary cultures of microglia

Our next aim was to address the physiological relevance of the finding of heteromers in a heterologous expression system. Accordingly, we performed assays to identify heteroreceptor complexes in in primary cultures of microglia. Proximity ligation assays (PLA) were performed using specific antibodies against cannabinoid CB_2 and GPR18 receptors (see Methods) and punctuated red marks were visualized surrounding DAPI-stained nuclei, demonstrating the existence of CB_2-GPR18 receptor complexes/clusters. The absence of the primary anti-GPR18 antibody led to a marked reduction of the PLA signal (Fig. 4A-B, untreated). To get insights into the functional role of CB_2R-GPR18 heteroreceptor complexes in microglial cells, cAMP intracellular levels and MAPK pathway activation were determined. In both assay types, treatment of microglia with JWH133 or PSBKK1415 induced a significant effect that was decreased when the cells were simultaneously treated with both ligands. Then, a negative cross-talk was also detected in primary cultures of microglia (Fig. 4D-E, untreated). Moreover, pretreatment of the primary cultures with the selective GPR18 antagonist PSBCB5 (1 μM) counteracted not only the PSBKK1415-induced ERK1/2 phosphorylation, but also the JWH133-induced effect. Cross-antagonism was also detected when SR144528 was used as it blocked both JWH133 and PSBKK1415 actions (Fig. 4E). Thus, cross-antagonism was also detected in resting microglia.

3.4. GPR18-CB_2R negative cross-modulation in activated microglia

It has been described that CB_2R expression increases in activated microglia and that the receptor then plays a relevant role in regulating the production of neuroinflammatory mediators (Pacher and Mechoulam, 2011; Navarro et al., 2018a). Our next aim was to assess the structural and functional implication of CB_2-GPR18 heteroreceptor complexes in primary

microglia activated by 48-h treatment with 1 μM LPS plus 200 U/mL IFN-γ (see (Navarro et al., 2018a)). The relative expression of transcripts for both CB_2R and GPR18 was analyzed by RT-PCR in microglia from wild type mice treated or not with LPS plus IFN-γ. mRNA specific for either CB_2R or GPR18 significantly increased in activated cells (Fig. 4C). By comparing microglial primary cultures treated or not with 1 μM LPS plus 200 U/mL IFN-γ, PLA results showed CB_2-GPR18 receptor heteromer expression in both resting and activated cells (Fig. 4A-B). We then determined the effect of agonists on cAMP levels and ERK1/2 phosphorylation. Interestingly, microglia treated with 1 μM LPS plus 200 U/mL IFN-γ showed an increase in CB_2R- and GPR18-induced signaling. The statistical analysis showed an interaction between cell activation (LPS plus IFN-γ) and receptor activation by agonists. While all the functional results showed a negative cross-talk, cross-antagonism (bidirectional) was identified in pERK but not in cAMP assays (Fig. 4D-E).

3.5. CB_2R-GPR18 heteromer expression and function assayed in primary microglia from $APP_{Sw,Ind}$ transgenic mice

Two-day-old pups obtained from $APP_{Sw,Ind}$ x WT mice crossings were individually genotyped and classified as non-transgenic (control) or heterozygous APP transgenic mice ($APP_{Sw,Ind}$). In adulthood the $APP_{Sw,Ind}$ mouse displays brain amyloid plaques and neuroinflammatory responses, including reactive microglia and cognitive deficits (Mucke et al., 2000). Primary cultures of microglia were prepared from both control and $APP_{Sw,Ind}$ mice. It should be noted that microglia from $APP_{Sw,Ind}$ do show an activated phenotype (see (Navarro et al., 2018a)).

To detect differential expression in CB_2-GPR18 receptor complexes in control and transgenic animals, PLA assays were developed using primary cultures of microglia obtained from control and $APP_{Sw,Ind}$ mice. Significant differences were found between wild-type and $APP_{Sw,Ind}$ mice both in the percentage of cells displaying red clusters (61% in control *vs* 73%

in $APP_{Sw,Ind}$ mice) and in the number of dots/cell in cells displaying dots (3.5 in control *vs* 5.0 in $APP_{Sw,Ind}$ mice) (Fig. 5A-B).

Cultures were also used to determine signaling upon agonist activation. We first analyzed the cAMP levels in forskolin-treated primary cultures of microglia from non-transgenic and $APP_{Sw,Ind}$ mice. Activation with the CB_2R selective agonist (JWH133, 300 nM) or with the GPR18 selective agonist (PSBKK1415, 100 nM) slightly decreased cAMP levels in microglia from controls, while it had a significantly higher effect on microglia from $APP_{Sw,Ind}$ mice (Fig. 5C). Interestingly, statistical analysis showed an interaction between mice genotype and agonist treatment. Simultaneous activation of the two receptors led to a negative cross-talk both in control and $APP_{Sw,Ind}$ animals (Fig. 5C). The effect of JWH133 on ERK1/2 phosphorylation was significantly higher in microglia from $APP_{Sw,Ind}$ and the analysis using two-way ANOVA showed an interaction between mice genotype and ligand treatment. When cells from $APP_{Sw,Ind}$ mice were pretreated with a CB_2R selective antagonist (SR144528, 1 µM) or with a GPR18 selective antagonist (PSBCB5, 1 µM), the effect of the two agonists was abolished, indicating a bidirectional cross-antagonism (Fig. 5D).

To sum up, activated microglia or microglia from $APP_{Sw,Ind}$ mice show an increase in the expression of CB_2R, GPR18, and CB_2R-GPR18 heteromers and a potentiation in specific signaling.

4. Discussion

Despite GPR18 and GPR55 may respond to cannabinoid molecules, the physiological role of the receptors and their signal transduction mechanisms are unclear. Neither they are real cannabinoid receptors nor share sequence similarity. Furthermore, pharmacological

characterization is very incomplete due to shortage in pharmacological tools. exist and v) the signal transduction mechanisms are not yet fully elucidated. In such a scenario, there is the possibility proven for GPR55 (Balenga et al., 2014; Martínez-Pinilla et al., 2014; Moreno et al., 2014) but not for GPR18 that these receptors may form heteromers with cannabinoid receptors. The consequences of heteroreceptor complex formation are multiple as it may result in cross-inhibition in some signaling pathways investigated in some expression system, but in potentiation in the case of activated microglia. In fact, CB_2R in resting microglia are not well coupled to G_i, whereas in activated cells, overexpressed CB_2R are robustly coupled to G_i and such finding correlates with a significant increase in the expression of CB_1R/CB_2R heteromers (Navarro et al., 2018a).

GPR55 may also form heteromers with either CB_1 or CB_2 receptors. Two different laboratories demonstrated that CB_2R may form heteromers with GPR55. In one of them the study of receptor heteromerization was linked to cancer because GPR55 is overexpressed in many cancerous cells (Moreno et al., 2014). The second paper showed heteromer formation and its signaling consequences in a heterologous expression system (Balenga et al., 2014). The presence of the partner receptor in the heteromer affected signal transduction from both CB_2R and GPR18. Co-expression of CB_2R and GPR55 led to a reduction in GPR55-mediated activation of transcription factors and DMR signal, while MAPK pathway activation was potentiated. When CB_2R activation was assayed, co-expression of CB_2R and GPR55 negatively modulated CB_2R-mediated MAPK pathway activation and DMR signals (Balenga et al., 2014). GPR55 may also form heteromers with CB_1R as reported from work not only in heterologous expression systems but in rodent and non-human primate models. A significant amount of CB_1-GPR55 heteroreceptor complexes are expressed in the corpus striatum of the rat, as demonstrated by detecting the heteromer print consisting of cross-antagonism, i.e. blockade of signaling of one receptor by the antagonist of the partner receptor in the

heteromeric complex. *In situ* PLA assays served to confirm expression of CB_1R-GPR55 complexes in the caudate and putamen nuclei of a non-human primate (Martínez-Pinilla et al., 2014).

The endocannabinoid system suffers profound changes in neurodegenerative diseases, especially in those with an inflammatory component (Bisogno and Di Marzo, 2010). CB_1R and CB_2R are both expressed in microglia, where CB_2R regulates CB_1R signaling, and under inflammatory conditions CB_2R expression and signaling are upregulated, and the negative cross-talk between CB_1R and CB_2R turns into synergy when both receptors are co-activated (Navarro et al., 2018a). (Walter et al., 2003) demonstrated that pathological stimulation of microglia triggered microglial cell migration by engaging CB_2R and receptors for abnormal cannabidiol, i.e. GPR18. GPR18 mRNA and protein expression was found in microglial cells, where NAGly, seemingly through GPR18, regulates migration and produces phenotypic switches, being a potent pro-migratory lipid (McHugh et al., 2010, 2012; McHugh, 2012).

We here show that GPR18 may interact with cannabinoid receptors but unlike GPR55, which may interact with both, GPR18 establishes receptor complexes with CB_2 but not with CB_1 receptors. This differential trend is relevant and shows that GPCR-GPCR interactions are not promiscuous, i.e. further to the need of being expressed in the same cell, the two interacting receptors should have complementary interfaces to be able to establish direct molecular contacts and display novel functional properties (Navarro et al., 2016, 2018b). The functionality of the CB_2R-GPR18 heteromer was studied in HEK-293T cells at the level of different signaling pathways. In all of them (intracellular cAMP accumulation, ERK1/2 phosphorylation and DMR), a negative cross-talk was detected, i.e. when both receptors are activated, the signal does not become additive but is reduced. The negative cross-talk, which may be considered a heteromer print, indicates that GPR18 activation places a brake to the action of cannabinoids acting on CB_2R.

As CB_2R is considered a receptor that may mediate neuroprotection (de Lago and Fernández-Ruiz, 2007; Sagredo et al., 2009; Gómez-Gálvez et al., 2016), microglia-expressed CB_2R-GPR18 receptor complexes may be targets for neuroprotection. In fact, the complex was expressed both in resting microglia and in primary cultures of microglia treated with 1 μM LPS plus 200 U/mL IFN-γ. Upon microglial activation CB_2R and GPR18 expression and signaling were upregulated, while the negative cross-talk was maintained. In AD and in the $APP_{Sw,Ind}$ mice AD model, inflammatory parameters are present in cortex and hippocampus (Mucke et al., 2000; Collins-Praino et al., 2014; Bronzuoli et al., 2016). Indeed the $APP_{Sw,Ind}$ model of AD has been described to display reactive astrocytes and activated microglia (Mucke et al., 2000; Saura et al., 2005). In the microglial cultures from of $APP_{Sw,Ind}$ mice brain, we found similar results to those obtained in microglia from wild-type animals treated with LPS/IFN-γ. Apart from the heteromer print, was found that the amount of CB_2R-GPR18 heteroreceptor complexes increased when compared to data generated using samples from control animals. All these data suggest that CB_2R-GPR18 complexes deserve attention as potential targets for the treatment of neuroinflammation occurring in neurodegenerative diseases.

Author contributions

This work is part of the PhD project of IRR, who performed many of the biophysical/biochemical and pharmacological assays and processed the resulting data, she wrote part of the methods section and edited the manuscript. GN designed and supervised the biophysical/biochemical and pharmacological assays and participated in manuscript preparation. DA performed the primary cultures of microglia and participated in some of the performed biophysical/biochemical and pharmacological assays. EIC provided statistical

guidance and participated in data analysis. MZ synthesized GPR18 ligands; KKK supervised the syntheses. CTS and CEM discovered, characterized, and designed the ligands for GPR18. CAS provided the transgenic animals and performed the genotyping. RF directed the work and coordinated the efforts of the participating laboratories. RF and CEM wrote the manuscript.

Competing interests

Authors declare no competing interests.

Acknowledgements

We would like to thank Prof. Martin Ríos for his help in statistical analysis of data and Jasmina Jiménez for technical help. This research was supported by grants (SAF2012-39875-C02-01 and SAF2016-80027-R) from the Spanish Ministry of Economy and Competitiveness (MINECO; grants may include EU FEDER funds) and from the Fundació La Marató de TV3 (grant number 201413330). Financial support by the Polish National Science Center DEC. 2013/11/B/NZ7/04865 is also acknowledged.

REFERENCES

Al Suleimani, Y.M., Al Mahruqi, A.S., 2017. The endogenous lipid N-arachidonoyl glycine is hypotensive and nitric oxide-cGMP-dependent vasorelaxant. Eur. J. Pharmacol. 794, 209–215. https://doi.org/10.1016/j.ejphar.2016.11.040

Balenga, N. a, Martínez-Pinilla, E., Kargl, J., Schröder, R., Peinhaupt, M., Platzer, W., Bálint, Z., Zamarbide, M., Dopeso-Reyes, I., Ricobaraza, a, Pérez-Ortiz, J.M., Kostenis, E., Waldhoer, M., Heinemann, a, Franco, R., 2014. Heteromerization of GPR55 and cannabinoid CB2 receptors modulates signaling. Br. J. Pharmacol. 1–64. https://doi.org/10.1111/bph.12850

Becker, A.M., Callahan, D.J., Richner, J.M., Choi, J., DiPersio, J.F., Diamond, M.S., Bhattacharya, D., 2015. GPR18 Controls Reconstitution of Mouse Small Intestine Intraepithelial Lymphocytes following Bone Marrow Transplantation. PLOS ONE 10, e0133854. https://doi.org/10.1371/journal.pone.0133854

Bilkei-Gorzo, A., 2012. The endocannabinoid system in normal and pathological brain ageing. Philos. Trans. R. Soc. Lond. B. Biol. Sci. 367, 3326–3341. https://doi.org/10.1098/rstb.2011.0388

Bisogno, T., Di Marzo, V., 2010. Cannabinoid receptors and endocannabinoids: role in neuroinflammatory and neurodegenerative disorders. CNS Neurol. Disord. Drug Targets 9, 564–573. https://doi.org/BSP/CDTCNSND/E-Pub/00056 [pii]

Bradshaw, H.B., Rimmerman, N., Hu, S., Benton, V.M., Stuart, J.M., Masuda, K., Cravatt, B.F., O'Dell, D.K., Walker, J.M., 2009. The endocannabinoid anandamide is a precursor for the signaling lipid N-arachidonoyl glycine by two distinct pathways. BMC Biochem. 10, 14. https://doi.org/10.1186/1471-2091-10-14

Bronzuoli, M.R., Iacomino, A., Steardo, L., Scuderi, C., 2016. Targeting neuroinflammation in Alzheimer's disease. J. Inflamm. Res. https://doi.org/10.2147/JIR.S86958

Burstein, S.H., McQuain, C.A., Ross, A.H., Salmonsen, R.A., Zurier, R.E., 2011. Resolution of inflammation by N-arachidonoylglycine. J. Cell. Biochem. 112, 3227–3233. https://doi.org/10.1002/jcb.23245

Cabral, G. a, Marciano-Cabral, F., 2005. Cannabinoid receptors in microglia of the central nervous system: immune functional relevance. J. Leukoc. Biol. 78, 1192–7. https://doi.org/10.1189/jlb.0405216

Caldwell, M.D., Hu, S.S.J., Viswanathan, S., Bradshaw, H., Kelly, M.E.M., Straiker, A., 2013. A GPR18-based signalling system regulates IOP in murine eye. Br. J. Pharmacol. 169, 834–843. https://doi.org/10.1111/bph.12136

Callén, L., Moreno, E., Barroso-Chinea, P., Moreno-Delgado, D., Cortés, A., Mallol, J., Casadó, V., Lanciego, J.L., Franco, R., Lluis, C., Canela, E.I., McCormick, P.J., 2012. Cannabinoid receptors CB1 and CB2 form functional heteromers in brain. J. Biol. Chem. 287, 20851–65. https://doi.org/10.1074/jbc.M111.335273

Collins-Praino, L.E., Francis, Y.I., Griffith, E.Y., Wiegman, A.F., Urbach, J., Lawton, A., Honig, L.S., Cortes, E., Vonsattel, J.P.G., Canoll, P.D., Goldman, J.E., Brickman, A.M., 2014. Soluble amyloid beta levels are elevated in the white matter of Alzheimer's patients, independent of cortical plaque severity. Acta Neuropathol. Commun. 2, 83. https://doi.org/10.1186/s40478-014-0083-0

Console-Bram, L., Brailoiu, E., Brailoiu, G.C., Sharir, H., Abood, M.E., 2014. Activation of GPR18 by cannabinoid compounds: a tale of biased agonism: GPR18 and intracellular calcium, MAPK, β-arrestin. Br. J. Pharmacol. 171, 3908–3917. https://doi.org/10.1111/bph.12746

de Lago, E., Fernández-Ruiz, J., 2007. Cannabinoids and neuroprotection in motor-related disorders. CNS Neurol. Disord. Drug Targets 6, 377–87. https://doi.org/10.2174/187152707783399210

España, J., Valero, J., Miñano-Molina, A.J., Masgrau, R., Martín, E., Guardia-Laguarta, C., Lleó, A., Giménez-Llort, L., Rodríguez-Alvarez, J., Saura, C.A., 2010. beta-Amyloid disrupts activity-dependent gene transcription required for memory through the CREB

coactivator CRTC1. J. Neurosci. Off. J. Soc. Neurosci. 30, 9402–9410. https://doi.org/10.1523/JNEUROSCI.2154-10.2010

Fernández-Ruiz, J., Romero, J., Velasco, G., Tolón, R.M., Ramos, J.A., Guzmán, M., 2007. Cannabinoid CB2 receptor: a new target for controlling neural cell survival? Trends Pharmacol. Sci. 28, 39–45. https://doi.org/10.1016/j.tips.2006.11.001

Finlay, D.B., Joseph, W.R., Grimsey, N.L., Glass, M., 2016. GPR18 undergoes a high degree of constitutive trafficking but is unresponsive to N-Arachidonoyl Glycine. PeerJ 4, e1835. https://doi.org/10.7717/peerj.1835

Franco, R., Fernández-Suárez, D., 2015. Alternatively activated microglia and macrophages in the central nervous system. Prog. Neurobiol. 131, 65–86. https://doi.org/10.1016/j.pneurobio.2015.05.003

Franklin, A., Stella, N., 2003. Arachidonylcyclopropylamide increases microglial cell migration through cannabinoid CB2and abnormal-cannabidiol-sensitive receptors. Eur. J. Pharmacol. 474, 195–198. https://doi.org/10.1016/S0014-2999(03)02074-0

Gantz, I., Muraoka, A., Yang, Y.K., Samuelson, L.C., Zimmerman, E.M., Cook, H., Yamada, T., 1997. Cloning and chromosomal localization of a gene (GPR18) encoding a novel seven transmembrane receptor highly expressed in spleen and testis. Genomics 42, 462–6. https://doi.org/10.1006/geno.1997.4752

Gómez-Gálvez, Y., Palomo-Garo, C., Fernández-Ruiz, J., García, C., 2016. Potential of the cannabinoid CB2 receptor as a pharmacological target against inflammation in Parkinson's disease. Prog. Neuropsychopharmacol. Biol. Psychiatry 64, 200–208. https://doi.org/10.1016/j.pnpbp.2015.03.017

Járai, Z., Wagner, J.A., Varga, K., Lake, K.D., Compton, D.R., Martin, B.R., Zimmer, A.M., Bonner, T.I., Buckley, N.E., Mezey, E., Razdan, R.K., Zimmer, A., Kunos, G., 1999.

Cannabinoid-induced mesenteric vasodilation through an endothelial site distinct from CB1 or CB2 receptors. Proc. Natl. Acad. Sci. U. S. A. 96, 14136–14141.

Jeong, H.-J., Vandenberg, R.J., Vaughan, C.W., 2010. N-arachidonyl-glycine modulates synaptic transmission in superficial dorsal horn: NAGly enhances glycine transmission in dorsal horn. Br. J. Pharmacol. 161, 925–935. https://doi.org/10.1111/j.1476-5381.2010.00935.x

Kohno, M., Hasegawa, H., Inoue, A., Muraoka, M., Miyazaki, T., Oka, K., Yasukawa, M., 2006. Identification of N-arachidonylglycine as the endogenous ligand for orphan G-protein-coupled receptor GPR18. Biochem. Biophys. Res. Commun. 347, 827–832. https://doi.org/10.1016/j.bbrc.2006.06.175

Lanciego, J.L., Barroso-Chinea, P., Rico, A.J., Conte-Perales, L., Callén, L., Roda, E., Gómez-Bautista, V., López, I.P., Lluis, C., Labandeira-García, J.L., Franco, R., 2011. Expression of the mRNA coding the cannabinoid receptor 2 in the pallidal complex of Macaca fascicularis. J. Psychopharmacol. Oxf. Engl. 25, 97–104. https://doi.org/10.1177/0269881110367732

Laprairie, R.B., Bagher, A.M., Kelly, M.E.M., Denovan-Wright, E.M., 2015. Cannabidiol is a negative allosteric modulator of the cannabinoid CB1 receptor. Br. J. Pharmacol. 172, 4790–4805. https://doi.org/10.1111/bph.13250

Lu, H.-C., Mackie, K., 2016. An Introduction to the Endogenous Cannabinoid System. Biol. Psychiatry 79, 516–525. https://doi.org/10.1016/j.biopsych.2015.07.028

Lu, V.B., Puhl, H.L., Ikeda, S.R., 2013. N-Arachidonyl glycine does not activate G protein-coupled receptor 18 signaling via canonical pathways. Mol Pharmacol 83, 267–82. https://doi.org/10.1124/mol.112.081182

Martínez-Pinilla, E., Reyes-Resina, I., Oñatibia-Astibia, A., Zamarbide, M., Ricobaraza, A., Navarro, G., Moreno, E., Dopeso-Reyes, I.G.G., Sierra, S., Rico, A.J.J., Roda, E.,

Lanciego, J.L.L., Franco, R., 2014. CB1 and GPR55 receptors are co-expressed and form heteromers in rat and monkey striatum. Exp. Neurol. 261, 44–52. https://doi.org/10.1016/j.expneurol.2014.06.017

Martínez-Pinilla, E., Varani, K., Reyes-Resina, I., Angelats, E., Vincenzi, F., Ferreiro-Vera, C., Oyarzabal, J., Canela, E.I., Lanciego, J.L., Nadal, X., Navarro, G., Borea, P.A., Franco, R., 2017. Binding and Signaling Studies Disclose a Potential Allosteric Site for Cannabidiol in Cannabinoid CB2 Receptors. Front. Pharmacol. 8, 744. https://doi.org/10.3389/fphar.2017.00744

Matouk, A.I., Taye, A., El-Moselhy, M.A., Heeba, G.H., Abdel-Rahman, A.A., 2017. The Effect of Chronic Activation of the Novel Endocannabinoid Receptor GPR18 on Myocardial Function and Blood Pressure in Conscious Rats. J. Cardiovasc. Pharmacol. 69, 23–33. https://doi.org/10.1097/FJC.0000000000000438

McHugh, D., 2012. GPR18 in microglia: Implications for the CNS and endocannabinoid system signalling. Br. J. Pharmacol. https://doi.org/10.1111/j.1476-5381.2012.02019.x

McHugh, D., Hu, S.S., Rimmerman, N., Juknat, A., Vogel, Z., Walker, J.M., Bradshaw, H.B., 2010. N-arachidonoyl glycine, an abundant endogenous lipid, potently drives directed cellular migration through GPR18, the putative abnormal cannabidiol receptor. BMC Neurosci. 11, 44. https://doi.org/10.1186/1471-2202-11-44

McHugh, D., Wager-Miller, J., Page, J., Bradshaw, H.B., 2012. siRNA knockdown of GPR18 receptors in BV-2 microglia attenuates N-arachidonoyl glycine-induced cell migration. J. Mol. Signal. 7, 10. https://doi.org/10.1186/1750-2187-7-10

Miller, S., Leishman, E., Oehler, O., Daily, L., Murataeva, N., Wager-Miller, J., Bradshaw, H., Straiker, A., 2016. Evidence for a GPR18 role in diurnal regulation of intraocular pressure. Invest. Ophthalmol. Vis. Sci. 57, 6419–6426. https://doi.org/10.1167/iovs.16-19437

Moreno, E., Andradas, C., Medrano, M., Caffarel, M.M., Pérez-Gómez, E., Blasco-Benito, S., Gómez-Cañas, M., Pazos, M.R., Irving, A.J., Lluís, C., Canela, E.I., Fernández-Ruiz, J., Guzmán, M., McCormick, P.J., Sánchez, C., 2014. Targeting CB2-GPR55 receptor heteromers modulates cancer cell signaling. J. Biol. Chem. 289, 21960–21972. https://doi.org/10.1074/jbc.M114.561761

Mucke, L., Masliah, E., Yu, G.Q., Mallory, M., Rockenstein, E.M., Tatsuno, G., Hu, K., Kholodenko, D., Johnson-Wood, K., McConlogue, L., 2000. High-level neuronal expression of abeta 1-42 in wild-type human amyloid protein precursor transgenic mice: synaptotoxicity without plaque formation. J. Neurosci. Off. J. Soc. Neurosci. 20, 4050–4058.

Navarro, G., Borroto-Escuela, D., Angelats, E., Etayo, Í., Reyes-Resina, I., Pulido-Salgado, M., Rodriguez-Perez, A.I., Canela, E.I., Saura, J., Lanciego, J.L., Labandeira-García, J.L., Saura, C.A., Fuxe, K., Franco, R., 2018a. Receptor-heteromer mediated regulation of endocannabinoid signaling in activated microglia. Role of CB1 and CB2 receptors and relevance for Alzheimer's disease and levodopa-induced dyskinesia. Brain. Behav. Immun. 67, 139–151. https://doi.org/10.1016/j.bbi.2017.08.015

Navarro, G., Cordomi, A., Brugarolas, M., Moreno, E., Aguinaga, D., Pérez-Benito, L., Ferre, S., Cortés, A., Casadó, V., Mallol, J., Canela, E.I., Lluis, C., Pardo, L., McCormick, P., Franco, R., 2018b. Cross-communication between Gi and Gs in a G-protein-coupled receptor heterotetramer guided by a receptor C-terminal domain. BMC Biology p.In the press.

Navarro, G., Cordomí, A., Zelman-Femiak, M., Brugarolas, M., Moreno, E., Aguinaga, D., Perez-Benito, L., Cortés, A., Casadó, V., Mallol, J., Canela, E.I., Lluís, C., Pardo, L., García-Sáez, A.J., McCormick, P.J., Franco, R., 2016. Quaternary structure of a G-

protein-coupled receptor heterotetramer in complex with Gi and Gs. BMC Biol. 14, 26. https://doi.org/10.1186/s12915-016-0247-4

Navarro, G., Hradsky, J., Lluís, C., Casadó, V., McCormick, P.J., Kreutz, M.R., Mikhaylova, M., 2012. NCS-1 associates with adenosine A(2A) receptors and modulates receptor function. Front. Mol. Neurosci. 5, 53. https://doi.org/10.3389/fnmol.2012.00053

Pacher, P., Mechoulam, R., 2011. Is lipid signaling through cannabinoid 2 receptors part of a protective system? Prog. Lipid Res. 50, 193–211. https://doi.org/10.1016/j.plipres.2011.01.001

Parmar, N., Ho, W.-S.V., 2010. N-arachidonoyl glycine, an endogenous lipid that acts as a vasorelaxant via nitric oxide and large conductance calcium-activated potassium channels: Vascular actions of N-arachidonoyl glycine. Br. J. Pharmacol. 160, 594–603. https://doi.org/10.1111/j.1476-5381.2009.00622.x

Penumarti, A., Abdel-Rahman, A.A., 2014. The Novel Endocannabinoid Receptor GPR18 Is Expressed in the Rostral Ventrolateral Medulla and Exerts Tonic Restraining Influence on Blood Pressure. J. Pharmacol. Exp. Ther. 349, 29–38. https://doi.org/10.1124/jpet.113.209213

Qin, Y., Verdegaal, E.M.E., Siderius, M., Bebelman, J.P., Smit, M.J., Leurs, R., Willemze, R., Tensen, C.P., Osanto, S., 2011. Quantitative expression profiling of G-protein-coupled receptors (GPCRs) in metastatic melanoma: The constitutively active orphan GPCR GPR18 as novel drug target. Pigment Cell Melanoma Res. 24, 207–218. https://doi.org/10.1111/j.1755-148X.2010.00781.x

Regard, J.B., Sato, I.T., Coughlin, S.R., 2008. Anatomical Profiling of G Protein-Coupled Receptor Expression. Cell 135, 561–571. https://doi.org/10.1016/j.cell.2008.08.040

Rempel, V., Atzler, K., Behrenswerth, A., Karcz, T., Schoeder, C., Hinz, S., Kaleta, K., Thimm, D., Kiec-Kononowiczb, K., Müller, C.E., 2014. Bicyclic imidazole-4-one

derivatives: a new class of antagonists for the orphan G protein-coupled receptors GPR18 and GPR55. Med Chem Commun 5, 632–649.

Sagredo, O., González, S., Aroyo, I., Pazos, M.R., Benito, C., Lastres-Becker, I., Romero, J.P., Tolón, R.M., Mechoulam, R., Brouillet, E., Romero, J., Fernández-Ruiz, J., 2009. Cannabinoid CB2 receptor agonists protect the striatum against malonate toxicity: Relevance for Huntington's disease. GLIA 57, 1154–1167. https://doi.org/10.1002/glia.20838

Saura, C.A., Chen, G., Malkani, S., Choi, S.-Y., Takahashi, R.H., Zhang, D., Gouras, G.K., Kirkwood, A., Morris, R.G.M., Shen, J., 2005. Conditional inactivation of presenilin 1 prevents amyloid accumulation and temporarily rescues contextual and spatial working memory impairments in amyloid precursor protein transgenic mice. J. Neurosci. Off. J. Soc. Neurosci. 25, 6755–6764. https://doi.org/10.1523/JNEUROSCI.1247-05.2005

Schoeder, C.T., 2017. Identification, optimization and characterization of pharmacological tools for the cannabinoid-activated orphan G protein-coupled receptor GPR18 and related receptors. PhD Thesis. University of Bonn. Bonn, Germany., Bonn, Germany.

Sierra, S., Luquin, N., Rico, A.J., Gómez-Bautista, V., Roda, E., Dopeso-Reyes, I.G., Vázquez, A., Martínez-Pinilla, E., Labandeira-García, J.L., Franco, R., Lanciego, J.L., 2015. Detection of cannabinoid receptors CB1 and CB2 within basal ganglia output neurons in macaques: changes following experimental parkinsonism. Brain Struct. Funct. 220, 2721–38. https://doi.org/10.1007/s00429-014-0823-8

Takenouchi, R., Inoue, K., Kambe, Y., Miyata, A., 2012. N-arachidonoyl glycine induces macrophage apoptosis via GPR18. Biochem. Biophys. Res. Commun. 418, 366–371. https://doi.org/10.1016/j.bbrc.2012.01.027

Vassilatis, D.K., Hohmann, J.G., Zeng, H., Li, F., Ranchalis, J.E., Mortrud, M.T., Brown, A., Rodriguez, S.S., Weller, J.R., Wright, A.C., Bergmann, J.E., Gaitanaris, G.A., 2003. The G protein-coupled receptor repertoires of human and mouse. Proc. Natl. Acad. Sci. 100, 4903–4908. https://doi.org/10.1073/pnas.0230374100

Walter, L., Franklin, A., Witting, A., Wade, C., Xie, Y., Kunos, G., Mackie, K., Stella, N., 2003. Nonpsychotropic cannabinoid receptors regulate microglial cell migration. J. Neurosci. Off. J. Soc. Neurosci. 23, 1398–405.

Yin, H., Chu, A., Li, W., Wang, B., Shelton, F., Otero, F., Nguyen, D.G., Caldwell, J.S., Chen, Y.A., 2009. Lipid G protein-coupled receptor ligand identification using β-arrestin PathHunter™ assay. J. Biol. Chem. 284, 12328–12338. https://doi.org/10.1074/jbc.M806516200

Figure legends

Figure 1. Molecular interaction between CB_2 and GPR18 receptors in living cells. Confocal microscopy images of HEK-293T cells transfected with CB_1R-YFP, CB_2R-YFP or GPR18-Rluc alone, or co-transfected with CB_1R-YFP and GPR18-Rluc or with CB_2R-YFP and GPR18-Rluc. GPR18 receptors (red) were identified by immunocytochemistry using anti-Rluc antibodies and CB_1R and CB_2R receptors (green) were identified by the fluorescence of YFP-containing fusion proteins (**A**). Co-localization is shown in the panels in the right (yellow). Cell nuclei were stained with Hoechst (blue channel). Scale bar: 10 µm. Correct functionality of the fusion proteins used in BRET assays assessed by intracellular cAMP determination assays (**B**). HEK-293T cells were transfected with cDNA encoding for CB_1R, CB_1R-YFP, CB_2R, CB_2R-YFP, GPR18 or GPR18-Rluc (1 µg cDNA) and cAMP production was determined after stimulation with 0.5 µM forskolin in the absence (100%) or presence of 200 mM ACEA (for CB_1R and CB_1R-YFP), 200 mM JWH133 (for CB_2R and CB_2R-YFP) or 30 nM PSBKK1415 (for GPR18 and GPR18-Rluc). Percentage of effect respect to the increase in cAMP levels achieved by 0.5 µM forskolin is represented. Results are the mean ± S.D. from 5 independent experiments performed in triplicates. No significant differences were found after Student's t test between effect in cells expressing the non-fused receptor or expressing the corresponding fusion protein. BRET saturation experiments performed using HEK-293T cells co-transfected with **(C):** GPR18-Rluc cDNA (1.6 µg) and increasing amounts of CB_1R-YFP cDNA (0 to 2 µg cDNA), **(D):** GPR18-Rluc cDNA (1.6 µg) and increasing amounts of CB_2R-YFP cDNA (0 to 2 µg cDNA), or **(E):** CB_1R-Rluc cDNA (1 µg) and increasing amounts of CB_2R-YFP cDNA (0 to 2.5 µg cDNA) as positive control (squares) and $GABA_B$-Rluc cDNA (0.5 µg) and increasing amounts of GPR18-YFP cDNA (0 to 3 µg cDNA) as a negative control (circles). The relative amount of BRET acceptor is given as the ratio between the fluorescence of the acceptor minus the fluorescence detected in cells only

expressing the donor and the luciferase activity of the donor (YFP/Rluc). BRET data are expressed as the mean ± S.D. of six different experiments performed in duplicates. mBU: milliBret units.

Figure 2. cAMP levels and pERK responses in single transfected cells. HEK-293T cells transfected with cDNA encoding for CB_2R **(A, C)** or GPR18 **(B, D)** were treated with increasing concentrations of JWH133 for CB_2R or PSBKK1415 for GPR18. cAMP accumulation **(A, B)** was detected by TR-FRET in the presence of 0.5 μM forskolin. cAMP production is expressed as % of levels obtained by 0.5 μM forskolin. ERK1/2 phosphorylation **(C, D)** was analyzed using an AlphaScreen®SureFire® kit (Perkin Elmer). ERK1/2 phosphorylation data are expressed as % respect to basal levels. Values are the mean ± S.D. of 5 different experiments performed in triplicates. One-way ANOVA followed by Bonferroni's multiple comparison *post hoc* test were used for statistical analysis. (**$p < 0.01$, ***$p < 0.001$; versus treatment with forskolin in cAMP or untreated cells in pERK assays).

Figure 3. Signaling in HEK-293T cells expressing CB_2R and/or GPR18. HEK-293T cells transfected with cDNA encoding for CB_2R **(A, D, G)**, for GPR18 **(B, E, H)** or both **(C, F, I)** were pre-treated with a selective receptor antagonist (1 μM SR144528 for CB_2R or 1 μM PSBCB5 for GPR18) and subsequently treated with selective agonists (100 nM JWH133 for CB_2R or 30 nM PSBKK1415 for GPR18), alone or in combination. cAMP accumulation **(A-C)** was detected by TR-FRET in the presence of 0.5 μM forskolin. cAMP production is expressed as % of levels obtained by 0.5 μM forskolin. ERK1/2 phosphorylation **(D-F)** was analyzed using an AlphaScreen®SureFire® kit (Perkin Elmer). ERK1/2 phosphorylation data are expressed as % respect to basal levels. In cAMP accumulation and MAPK signaling assays, values are the mean ± S.D. of 8 different experiments performed in triplicates, and

one-way ANOVA followed by Bonferroni's multiple comparison *post hoc* test were used for statistical analysis. (*p < 0.05, **p < 0.01, ***p < 0.001; versus treatment with forskolin in cAMP or basal in pERK assays). (##p < 0.01, ###p < 0.001; versus treatment with JWH133 alone). (&p < 0.05, &&p < 0.01, &&&p < 0.001; versus treatment with PSBKK1415 alone). **(G-I):** DMR tracings representing the picometer-shifts of reflected light wavelength (in pm) over time upon ligand treatment: JWH133 (red), PSBKK1415 (dark blue), JWH133 + PDBKK1415 (purple), SR144528 + JWH133 (pink), SR144528 + PSBKK1415 (orange), PSBCB5 + JWH133 (green), PSBCB5 + PSBKK1415 (light blue).

Figure 4. Detection of the CB_2-GPR18 receptor heteromers in primary microglial cultures. Proximity Ligation Assay (PLA) was performed as described in Methods in primary cultures of microglial cells incubated for 48 h in the absence or presence of 1 μM LPS and 200 U/mL IFN-γ using specific primary antibodies against CB_2R and GPR18. Representative images corresponding to stacks of 5 sequential planes are shown in **A**. Cell nuclei were stained with Hoechst (blue) and heteroreceptor clusters appear as red dots. Scale bar: 20 μm. (**B**): Ratio (r; number of red spots/cell-containing spots) and percentage of cells containing one or more red spots (numbers above each bar) are the mean ± S.D. of counts in 4 different fields from every sample (n=5). No significant differences were found between untreated (white bars) and LPS plus IFN-γ (black bars) conditions neither in the number of red spots/cell-containing spots nor in the percentage of cells containing one or more red spots. Primary cultures of microglia were incubated for 48 h with medium or with medium containing 1 μM LPS and 200 U/mL IFN-γ (**C**). Relative gene expression of CB_2R and GPR18 was measured by real time-PCR. Data represent $2^{-\Delta\Delta Ct}$, and data are the mean ± S.D. of 6 different experiments (different cell cultures) performed in triplicates. Student's t-test (paired) was used for statistical analysis. (*p < 0.05, **p < 0.01; versus untreated). Primary

cultures of microglia were incubated for 48 h with medium (white bars) or with medium containing 1 μM LPS plus 200 U/mL IFN-γ (black bars). Cells were then pre-treated with selective receptor antagonists (1 μM SR144528 for CB_2R or 1 μM PSBCB5 for GPR18) and subsequently treated with selective agonists (100 nM JWH133 for CB_2R or 30 nM PSBKK1415 for GPR18), alone or in combination. cAMP accumulation **(D)** was detected by TR-FRET in the presence of 0.5 μM forskolin. cAMP production is expressed as % of levels obtained by 0.5 μM forskolin. ERK1/2 phosphorylation **(E)** was analyzed using an AlphaScreen®SureFire® kit (Perkin Elmer). ERK1/2 phosphorylation data are expressed as % respect to basal levels. Panels **D, E**: Values are the mean ± S.D. of 6 different experiments performed in triplicates. Two-way ANOVA for factors ligand and resting/LPS plus 200 U/mL IFN-γ showed statistical differences (#$p < 0.05$, ###$p < 0.001$). One-way ANOVA followed by Bonferroni's multiple comparison *post-hoc* test showed statistical differences: individual treatment versus 0.5 μM forskolin in cAMP or versus basal in pERK (*$p < 0.05$, ***$p < 0.001$), or combined versus individual treatment (&$p < 0.05$, &&&$p < 0.001$).

Figure 5. CB_2-GPR18 receptor heteromer expression and function in primary cultures of microglia from the $APP_{Sw,Ind}$ mice. Proximity Ligation Assay (PLA) was performed as described in Methods in primary cultures of microglia cells from two-day-old wild-type (control) and $APP_{Sw,Ind}$ mice using specific primary antibodies against CB_2R and GPR18. Representative images corresponding to stacks of 5 sequential planes are shown **(A)**. Cell nuclei were stained with Hoechst (blue) and heteroreceptor complexes appear as red dots. Scale bar: 20 μm. **(B)** Ratio (r; number of red spots/cell-containing spots) and percentage of cells containing one or more red spots (numbers above each bar graphs) are the mean ± S.D. of counts in 4 different fields from every sample (n=5). Two-way ANOVA for factors red dots and control (white bars)/$APP_{Sw,Ind}$ (black bars) showed statistical differences (#$p < 0.05$).

Panels **C, D:** Primary cultures of microglial cells of two-day-old wild-type (control, white bars) and $APP_{Sw,Ind}$ (black bars) mice were pre-treated with selective receptor antagonists (1 μM SR144528 for CB_2R or 1 μM PSBCB5 for GPR18) and subsequently treated with selective agonists (300 nM JWH133 for CB_2R or 100 nM PSBKK1415 for GPR18), alone or in combination. cAMP accumulation **(C)** was detected by TR-FRET in the presence of 0.5 μM forskolin. cAMP production is expressed as % of levels obtained by 0.5 μM forskolin. ERK1/2 phosphorylation **(D)** was analyzed using an AlphaScreen®SureFire® kit (Perkin Elmer) ERK1/2 phosphorylation data are expressed as % respect to basal levels. Values are the mean ± S.D. of 6 different experiments performed in triplicates. Two-way ANOVA for factors ligand and control/$APP_{Sw,Ind}$ showed statistical differences (#$p < 0.05$, ###$p < 0.001$). One-way ANOVA followed by Bonferroni's multiple comparison *post-hoc* test showed statistical differences: individual treatment versus 0.5 μM forskolin in cAMP or versus basal in pERK (***$p < 0.001$) or combined versus individual treatment (&$p < 0.05$, &&$p < 0.01$, &&&$p < 0.001$).

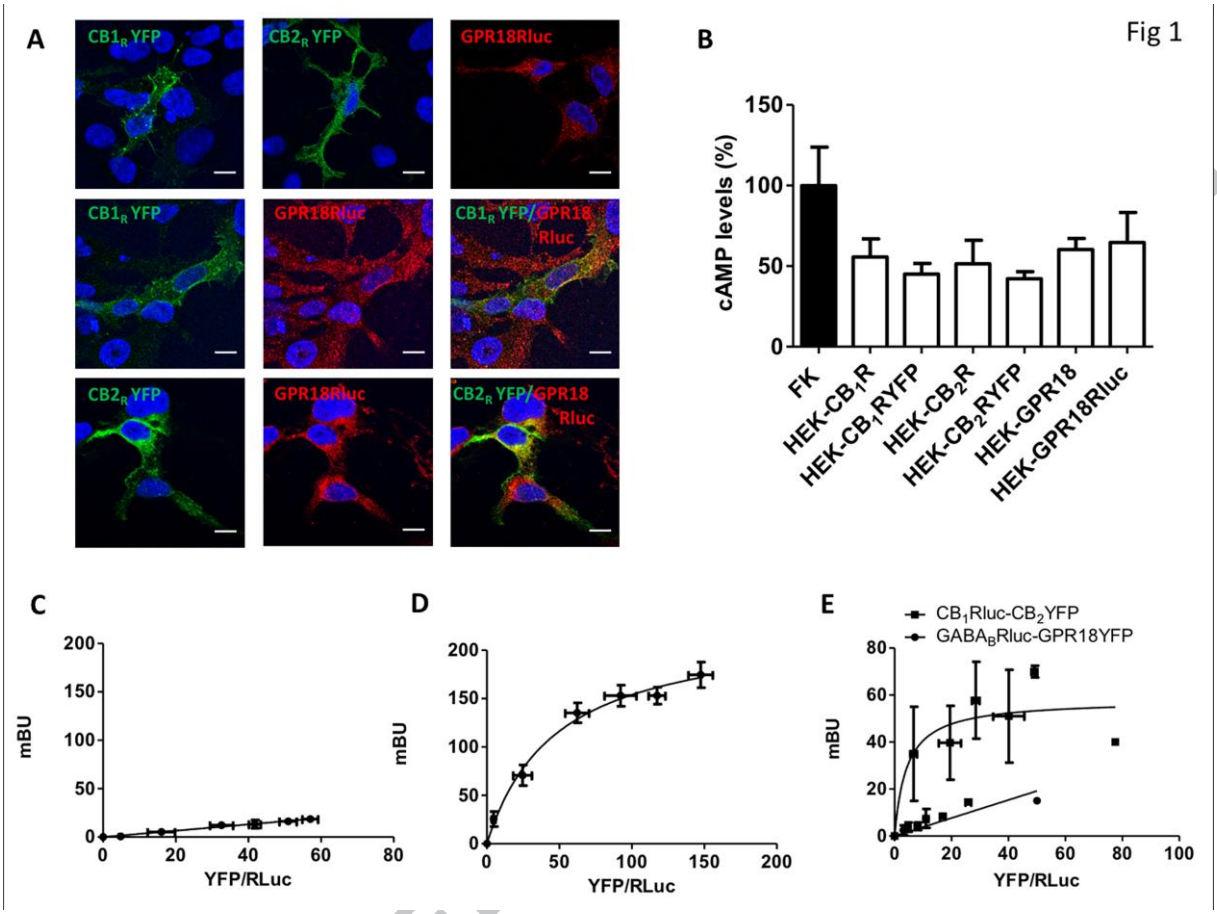

Fig 2

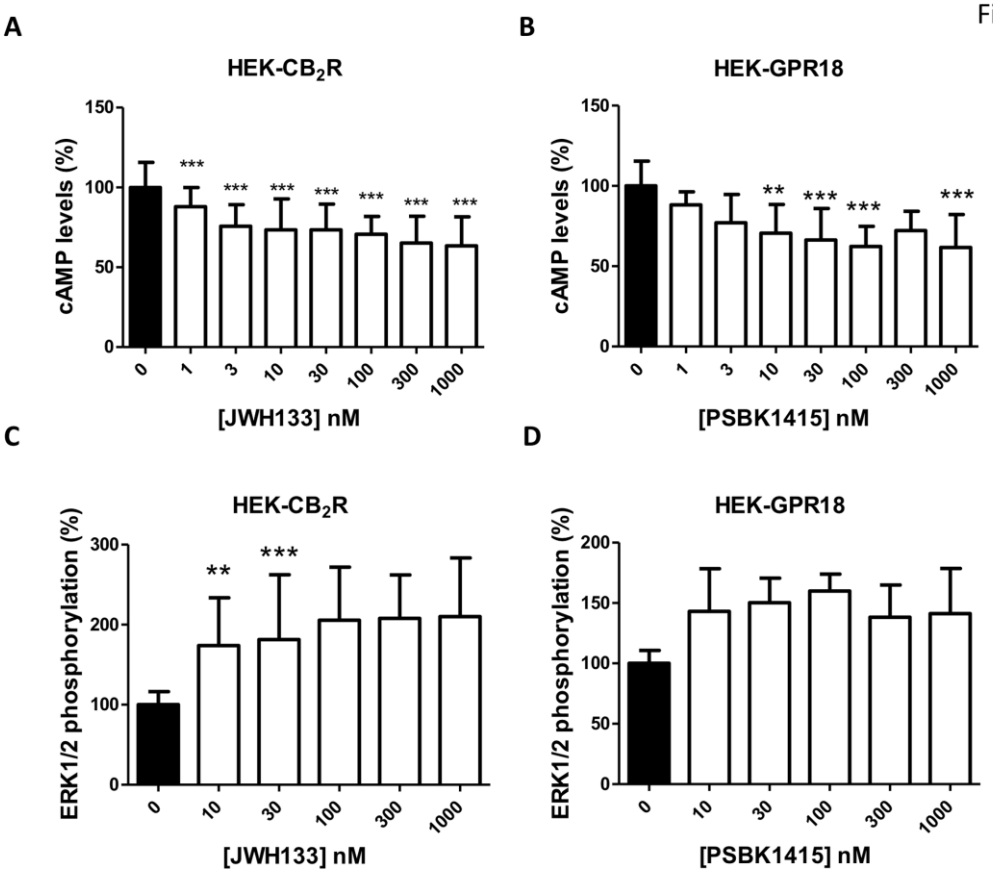

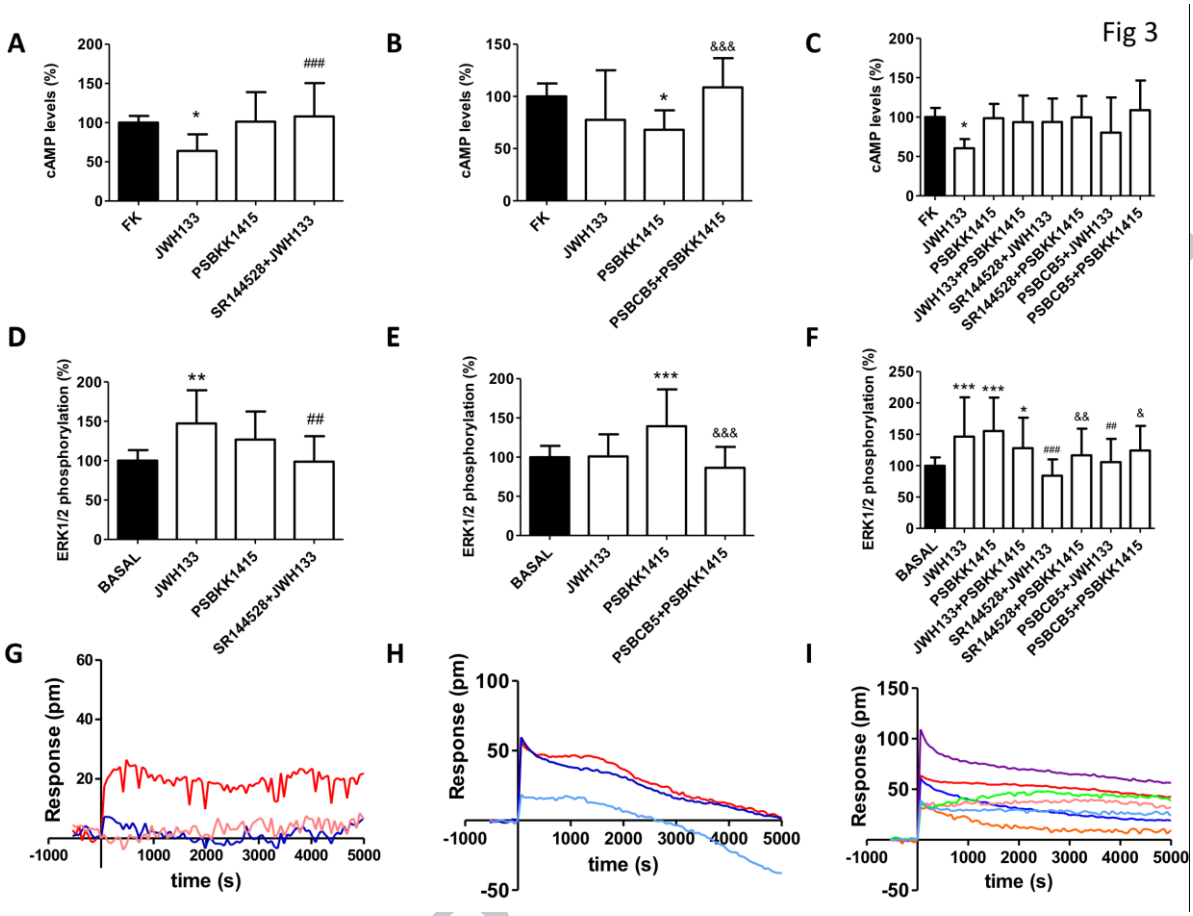

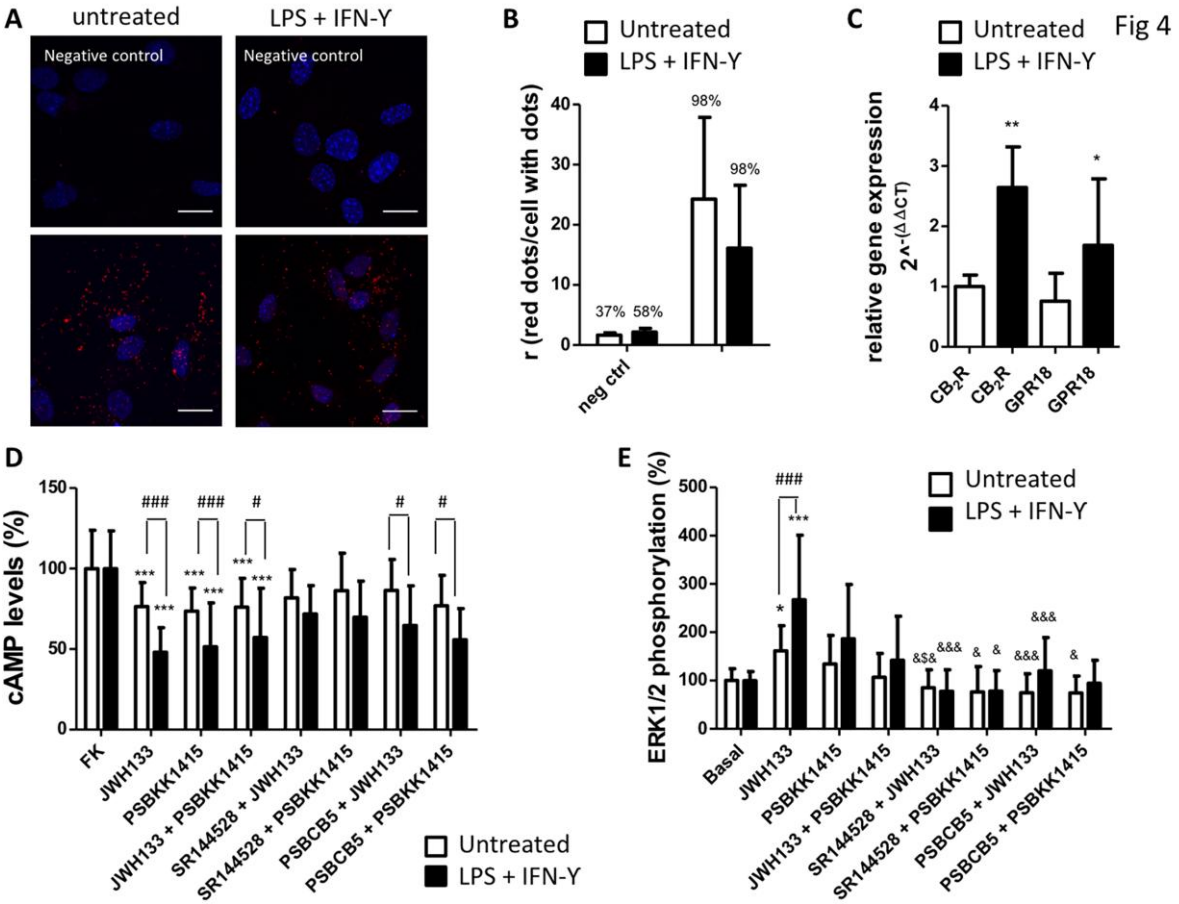

Fig 4

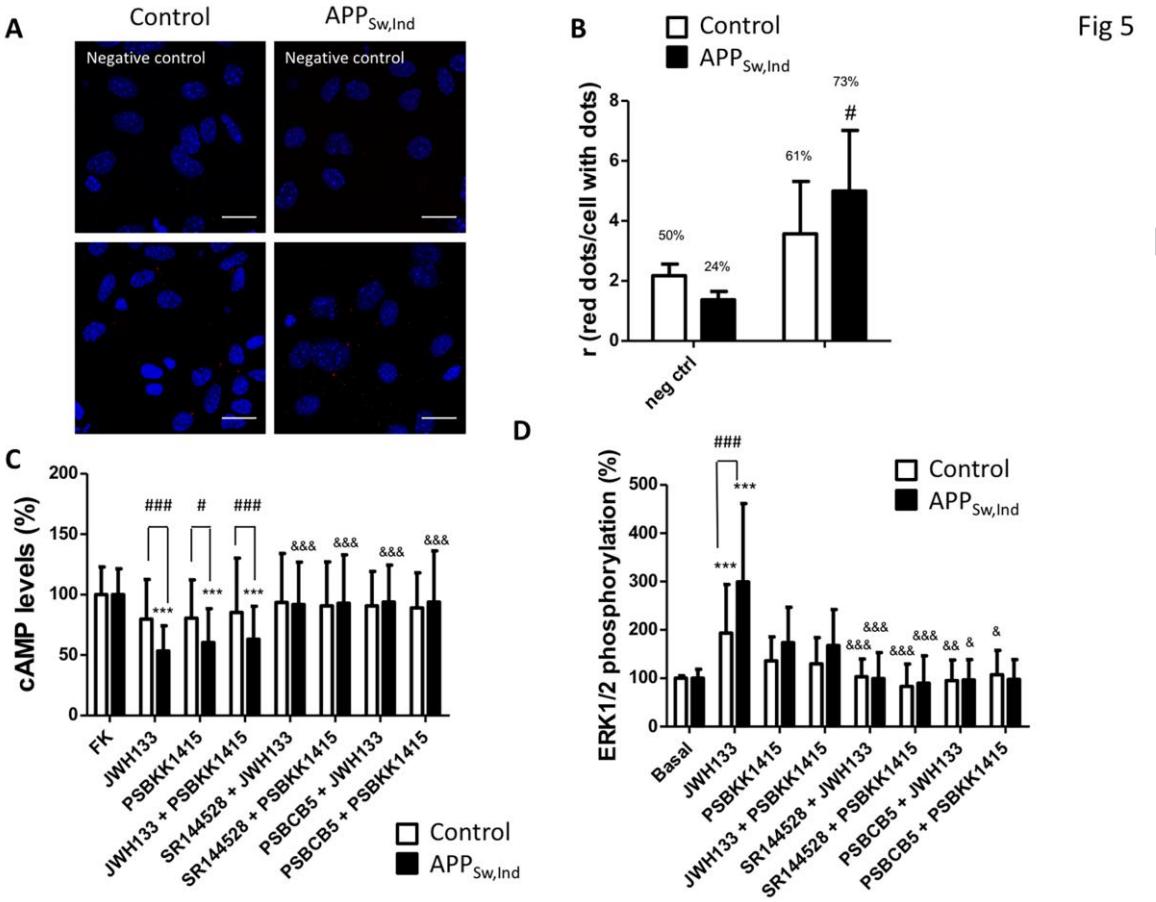

Fig 5

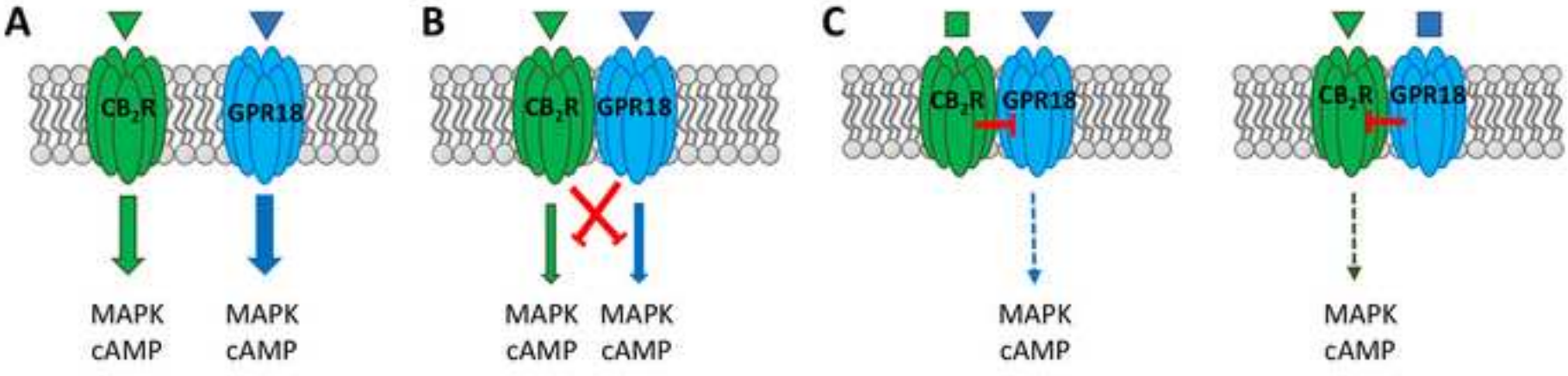

Graphical Abstract. Signaling (A) in CB_2R/GPR18 heteromers, is regulated by cross-regulation: coactivation reduces signaling (B) and there is bidirectional cross-antagonism i.e. one antagonist of blocks activation of partner receptor (C).